Vol. 21, No. 2(2022) Proc2623
Revista Mexicana de Ingeniería Química

Effect of drying on the extraction yield of *Luma chequen* (*Molina*) *A. Gray* essential oil

Efecto del secado en el rendimiento de la extracción de aceite esencial de *Luma chequen* (*Molina*) *A. Gray*

M.E. Borja-Málaga[1], A. Jiménez-Ochoa[1], E. Medina-de Miranda[1]*, F.A. Escobedo-Vargas[2]

[1] *Universidad Nacional de San Agustín de Arequipa, Facultad de Ingeniería de Procesos, Laboratorio de Operaciones Unitarias - Área de Investigación en Ingeniería, Av. Independencia s/n, Arequipa, Perú.*
[2] *School of Chemical & Biomolecular Engineering, Cornell University, Ithaca, NY 14953, USA*

Received: October 25, 2021; Accepted: April 13, 2022

Abstract

This work studies the effect of drying at 40 °C of the leaves and stems of the species *Luma chequen* (*Molina*) *A. Gray* on the extraction yield of its essential oil by steam distillation at a pilot scale. From the micromorphological evaluation at the moisture levels fresh state (72±1%), critical moisture (24±1%) and equilibrium moisture (8.2±0.5%), it is found that the tissues fold, the secretory cavities thin out, according to the lacunarity, the microstructure of the plant material exhibits greater uniformity at the critical moisture. For the extraction tests 18 levels of moisture were considered, keeping the packing factor at 54 Kg/m^3. The maximum yield of 0.52 ± 0.01% (v/w) was reached when the moisture of the material was 22±1%, very close to the critical moisture. A first-order model provided a suitable fit to the extraction kinetic data for samples with different humidity levels. Based on the evaporation rate equation, a description of the microstructure of the material and the drying conditions, a model was developed which shows the evaporation mechanism to be dominant in both the drying process and in the extraction of essential oil.

Keywords: drying, *Luma chequen*, micromorphology, oil essential, yield.

Resumen

El presente estudio evaluó el efecto del secado a 40°C, de las hojas y tallos jóvenes de la especie *Luma chequen* (*Molina*) *A. Gray*, en el rendimiento de la extracción de su aceite esencial por arrastre de vapor a nivel piloto. De la evaluación micromorfológica en los niveles de humedad; estado fresco (72±1%), humedad crítica (24±1%) y la humedad de equilibrio (8.2±0.5%), se evidenció plegamiento de los tejidos y adelgazamiento de las cavidades secretoras, la dimensión fractal fue relativamente constante (2.1) y según la lacunaridad, se tuvo mayor uniformidad en la microestructura del material vegetal a la humedad crítica. Para las pruebas de extracción se consideraron 18 niveles de humedad, manteniendo el factor de empaquetamiento en 54 Kg/m^3. Se alcanzó el máximo rendimiento de 0.52 ± 0.01% (*v/p*), cuando la humedad del material fue 22±1%, muy próxima a la humedad crítica. Las curvas cinéticas de extracción para diferentes niveles de humedad se ajustan adecuadamente a un modelo de primer orden. Basado en la ecuación de velocidad de evaporación, las condiciones tanto de la microestructura del material como las del secado, se dedujo un modelo que muestra al mecanismo de evaporación, como el gobernante en el proceso de secado y en la extracción del aceite esencial.

Palabras clave: aceite esencial, *Luma chequen*, micromorfología, rendimiento, secado.

* *Corresponding author. E-mail*: emedinale@unsa.edu.pe
https://doi.org/10.24275/rmiq/Proc2623
ISSN:1665-2738, *issn-e*: 2395-8472

1 Introduction

Luma chequen (*Molina*) *A. Gray* is a species within the genus *Luma* and *Myrtaceae* family. It grows between 2500 and 4000 meters ASL in the region of Arequipa, Peru. This plant may be found in inter-Andean valleys because it is capable of adapting to humid and sandy soils (Reynel and Marcelo, 2009; Sotta, 2000). Its essential oil has antioxidant, antibacterial and fungicide properties (Cabrera, 2019; Carhuapoma *et al*., 2006; Fernández, 2019; Gonçalves *et al*., 2011; Moina, 2015). This is found in internal secretion structures of its leaves, stems and flowers, specifically in secretory cavities of the schizolysigenic type (Ciccarelli *et al*., 2008; Retamales and Scharaschkin, 2015).

While new methods have been developed to extract essential oils (Dima and Dima, 2015; Stratakos and Koidis, 2016) which can potentially provide improved yield, product quality or reduced energetic demands (Kusuma and Mahfud, 2017; Kusuma and Mahfud, 2018), steam distillation is still the standard method for such extractions at large scales due to its lower costs of installation, operation and maintenance (Masango,2005; Talati, 2012). Steam distillation has been effectively used before for the extraction of the essential oil of *Luma chequen* (Fernández, 2019; Moina, 2015; Ruíz *et al*., 2015) because of such suitable characteristics of the species as high permeability, access to cellular cavities, and humidity content (Berka *et al*., 2010; Talati, 2012).

The moisture content of the raw material may have an important effect on the extraction yield; therefore, a dehydration pre-treatment is recommended (Moreno, 2010). From the different methods available, drying with warm air best preserves the volatile components contained in the vegetable material (An *et al*., 2016); however, the parameters of the material should be considered -the microstructure and distance the internal liquid takes to reach the surface- as well as parameters of the drying air-temperature, humidity, velocity and the direction of flow. (Dávila, 2004; McCabe and Smith, 2007). The drying velocity is constant until the critical moisture content is reached. Hereafter, the internal migration of water from the interior towards the surface of the material decreases and stabilizes at the equilibrium moisture, where the vapor pressure of the liquid inside material is equal to the partial pressure of the vapor in the gaseous state (Freire *et al*., 2012). During drying, the loss of water and volatiles results in important structural changes in the materials, such as shrinkage due to the reduction of their cellular dimensions. This shrinkage affects the heat and mass transfer parameters, and it can be evaluated from the micromorphology of the materials that are subjected to drying. The estimation of these microstructural alterations can be carried out using Euclidean Geometry, which evaluates entire dimensions of objects; and Fractal Geometry, that models the irregular components of the microstructure (Muchtar *et al*., 2016; Ramos *et al*., 2003; Santacruz *et al*., 2008); this is based on parameters of fractal dimension (measure of the complexity or heterogeneity of spatial arrangements) and lacunarity (measure of the distribution of empty spaces) (Azor, 2016).

In drying, the predominant mechanisms in the transport of moisture from the interior to the surface of the material are liquid diffusion, vapor diffusion, liquid flow, and vapor flow; all of them often included within an effective diffusivity parameter, which is evaluated in the modeling of the drying process of various materials. The effects of drying phenomena cannot be generalized for biological materials because they have particular characteristics associated with properties that can undergo significant alterations during dehydration (Freire *et al*.,2012; Salcedo *et al*.,2016), which will alter the mass transfer rate of the volatile components when the dried materials are subjected to a subsequent extraction of their essential oils. It is due to this fact that the objective of this study is to evaluate the effect of drying on leaves and young stems of *Luma chequen* (*Molina*) *A. Gray* in terms of the extraction yield of essential oil produced by steam distillation at pilot scale, supported by the micromorphology of the vegetable material.

2 Materials and methods

The vegetable material (leaves and young stems) was collected from the gardens of the National University of Saint Agustin of Arequipa (UNSA), from December (2019) to December (2021). The material was technically identified as *Luma chequen* (*Molina*) *A. Gray*, as stated in the certificate N° 081A-2018 issued by the *Herbario Arequipense* (HUSA).

2.1 *Drying process*

The moisture content of the materials was determined according to the standard NMX-F-428-1982 by means of a moisture analyzer (OHAUS MB90, USA). The drying process took place in the automatic forced flux convective dryer (A&C Ingenieros, Perú), at 40 °C (Boutebouhart *et al.*, 2019; Vieira de Souza *et al.*, 2016). The moisture content percentage on a wet basis was calculated as shown in Eq. (1):

$$X_{\text{wet basis}} = \frac{w_1 - w_2}{w_1} \times 100\% \quad (1)$$

where, w_1 is initial weight of the sample, g; and w_2 is weight of the sample after drying, g.

2.2 *Essential oil extraction*

The pilot plant for the extraction of essential oil by steam distillation was deployed, model EM15 *A&C Ingenieros* (Perú), in stainless steel AISI 304, located at the Laboratory of Unitary Operations at the UNSA. In this process, the extractor (with a chamber capacity of 12.6 L) is preheated, making steam circulate to distribute the previously chopped vegetable material (3 to 6 mm) into a metallic support provided with three plates, each one has a stainless-steel mesh at the base to allow the vapor flow. The saturated vapor generated in the electric boiler is injected from the bottom part of the extractor, interacting with the vegetable material, and, thus, extracting the essential oil. Then, the mixture of steam and essential oil goes to a vertical condenser (a shell and tube condenser) and is collected in a gravity separator (Florentine) connected to a cold bath at 4 °C to improve the separation between essential oil and hydrolate (Chávez *et al.*, 2018) (Figure 1).

To evaluate the effect of moisture of the raw material on the yield of the extraction, 18 tests by triplicate with 700g of material were run, varying moisture in intervals of 4%, within the range of the fresh moisture (Xfresh = 72%) and the equilibrium moisture (Xeq = 8%), as shown in Table 1.

The water vapor input pressure in the extractor was held constant at 34.5 kPa (Montoya, 2010), the total time of extraction was 40 minutes and the packing factor (PF) calculated using Eq. (2), was held constant at 54 Kg/m^3 (Moghrani and Maachi, 2008; Rezzoug *et al.*, 2005):

$$PF = \frac{W_{VM}}{V_{EC}} \quad (2)$$

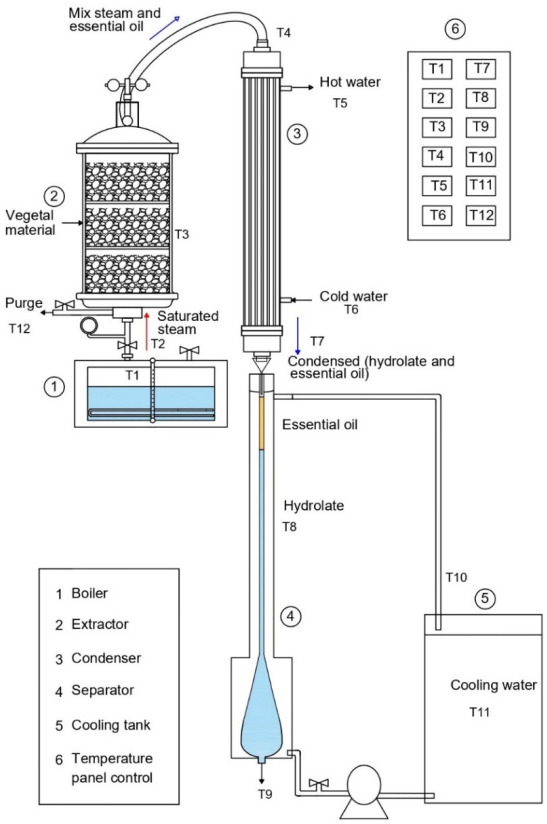

Fig. 1. Diagram of the steam distillation equipment for essential oil.

Table 1. Experimental design for the evaluation of the effect of moisture on extraction yield.

Essay N°	Moisture (%)	Essay N°	Moisture (%)
1	Xfresh	**10**	38
2	70	**11**	34
3	66	**12**	30
4	62	**13**	26
5	58	**14**	22
6	54	**15**	18
7	50	**16**	14
8	46	**17**	10
9	42	**18**	Xeq

where, W_{VM} weight of vegetable material, kg; and V_{EC} is volume of extractor chamber, m^3.

2.3 *Histological method*

The leaves and the stems were wrapped in paraffin and cut into histological sections of 5 μm, utilizing the rotation microtome RM2125RT (Leica, Germany),

followed by dewaxing and rinsing in xylol. The histochemical staining of the cuts was conducted using the method of hematoxylin and eosin. The mounting was performed with Canadian balsam (Arenas, 2010; Prophet *et al*., 1995). The sections of leaves and stems were observed using the optical microscope DM 500 (Leica, Germany). All chemical reagents were purchased from Merck Laboratories (Darmstadt, Germany).

2.4 Estimation of microstructural changes

2.4.1 Size estimation of secretory cavities

Ten samples were considered for each moisture level (fresh moisture, critical moisture and equilibrium moisture). Then, using the LAS EZ Leica Application Suite v 3.4 software, measurements were taken of the major and minor diameters of all secretory cavities observed in the images captured by the model ICC50 camera of the optical microscope DM 500 (Leica, Germany).

2.4.2 Lacunarity

To calculate lacunarity, the gliding box method was used (Allain and Cloitre, 1991). For this, the images obtained from the optical microscope were converted to binary data using the graythresh and im2bw tools of the Matlab software. The box size (r) was varied from 10 to 90 pixels in intervals of 20. The box of size r was slid through the binary matrix of the image and the box mass was calculated (sum of the sliding box).

2.5 Chemical analysis of essential oil (CG-MS)

The analysis of the essential oil sample composition from the vegetable materials with optimal moisture content was carried out at the mass chromatographer and spectrophotometer of the Universidad Industrial de Santander, Colombia. The analysis was performed according to the standard ISO 7609-1985 (E): *Essential oils - Analysis by gas chromatography on capillary columns - General method*. The gas chromatograph AT 6890 Series Plus (Agilent Technologies, Palo Alto, California, USA), coupled to a selective mass detector (Agilent Technologies, MSD 5975), and the gas chromatograph AT 7890 GC System (Agilent Technologies, Palo Alto, California, USA), coupled to a mass selective detector (Agilent Technologies, MSD 5975C) operated in the full frequency scan mode (*full scan*) and were set for the identification of polar and non-polar components of the sample. The columns deployed in the analysis where DB-SMS (apolar) (J& W Scientific, Folsom, CA, USA) [5%-phenyl-poly (dimethyl siloxane), 60 m x 0,25 mm x 0,25 μm] and DB-WAX (polar) (J& W Scientific, Folsom, CA, USA) [Poly (ethylene glycol), 60 m $\times$ 0.25 mm $\times$ 0.25 μm]. The injection was performed in split mode (30:l), Vny = 2μL.

3 Results and discussion

3.1 Kinetics of the drying process

The kinetics of the drying process in the automatic convective dryer with forced flow at 40°C is shown in Figure 2. Period of constant drying rate can be identified until reaching the range of 24±1%, which corresponds to the critical moisture (Xcr); and of decreasing rate, where the equilibrium moisture (Xeq) falls between the values of 8.2±0.5%. Based on the equations corresponding to the drying periods (Figure 2), the drying times were determined for the different moisture levels considered in the extraction tests (Figure 8).

3.2 Evaluation of microstructural changes in leaves and young stems of Luma chequen (Molina) A. Gray

The micromorphology of the young leaves and stems was evaluated at the moisture levels corresponding to the fresh state, critical moisture, and equilibrium moisture, determined in the previous section, in the sense of observing the microstructural changes caused by the loss of water and volatile components.

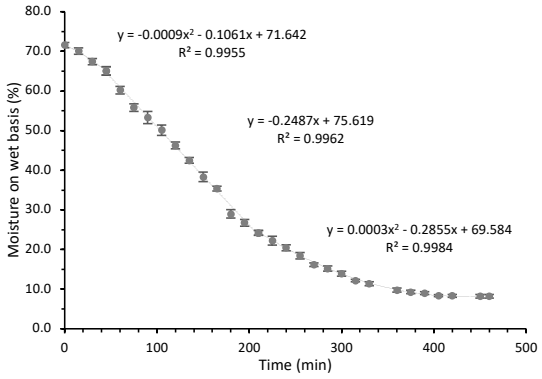

Fig. 2. Drying curve of leaves and young stems of *Luma chequen* (*Molina*) *A. Gray* in convective dryer at 40°C.

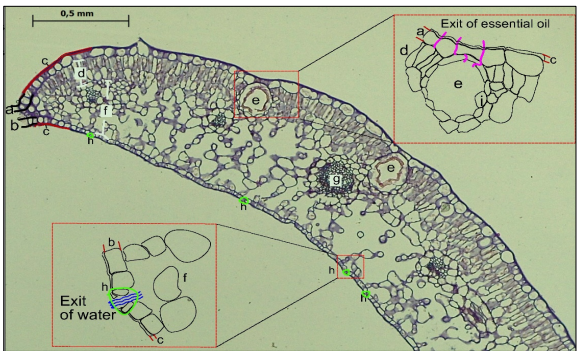

Fig. 3. Exit mechanism of essential oil and water in the leave of *Luma chequen* (*Molina*) *A. Gray* in fresh state (72%). Cross section at 50 μm, hematoxylin and eosin staining. a.adaxial epidermis. b. abaxial epidermi. c. cuticle. d. Palisade parenchyma. e. esquizolisigenous cavity. f. spongy parenchyma. g. vascular bundies. h. stomata. i. epithelial cells.

For this, it becomes necessary to understand the outlet mechanisms of both of these components. In this regard, it is known that the liberation of essential oil from the secretory cavities happens predominantly through the coating of cells most proximate to the cuticle and that the outlet of water contained in intercellular gaps is ejected mainly through the stomata, but smaller quantities of water are expelled through the cuticle (Alves de Assis *et al*., 2020). Therefore, regarding the *Luma chequen* it is expected for the water loss to be given in greater measure through the abaxial epidermis (underside) of the leave, where the stomata is located (Retamales and Scharaschkin, 2015), as shown in Figure 3.

In the transverse cross sections views of the fresh leaf at 72% moisture, the secretory cavities were mostly in contact with the adaxial epidermis (the beam) behind the cells of the palisade parenchyma. In some cases, they were also in contact with the abaxial epidermis (the underside). In this side, the cavities may be affected by the proximity to the stomata, where greater water loss occurs.

Even though drying at 40°C preserves volatile components, the cavities nearest to the adaxial side (the overside) may lose part of their most volatile components, as occurs with monoterpenes, which, according to Guenther *et al*. (1991), are emitted mostly from the adaxial side.

As moisture decreases, the palisade parenchyma and the spongy are fold towards the epidermis (Figures 4B y 4C) due to the reduction in size of the cells of which they are composed. This folding results in the cavities being closer to the surface, as observed in Figures 4B (24% moisture) and 4C (8% moisture). Nevertheless, in the latter case, cell collapse can be observed, which would lead to the tearing of secretory cavities, liberating the essential oil with greater ease through the cuticle without the need for a driving force. This could produce a substantial loss of essential oil prior to extraction.

Based on the measurements made with the LAS EZ Leica Application Suite v 3.4 software of the secretory cavities at the 3 moisture levels, the size distribution was obtained and evaluated in 10 μm intervals (Figure 5).

As can be seen, in Figures 5A, 5B and 5C, the distribution of larger diameters shifts to lower values as the moisture of the plant material decreases, and not presenting cavities with the largest diameters, from 121 to 140 μm. Similarly, the frequencies in the ranges from 71 to 110 μm, become more uniform in the 8% moisture sample.

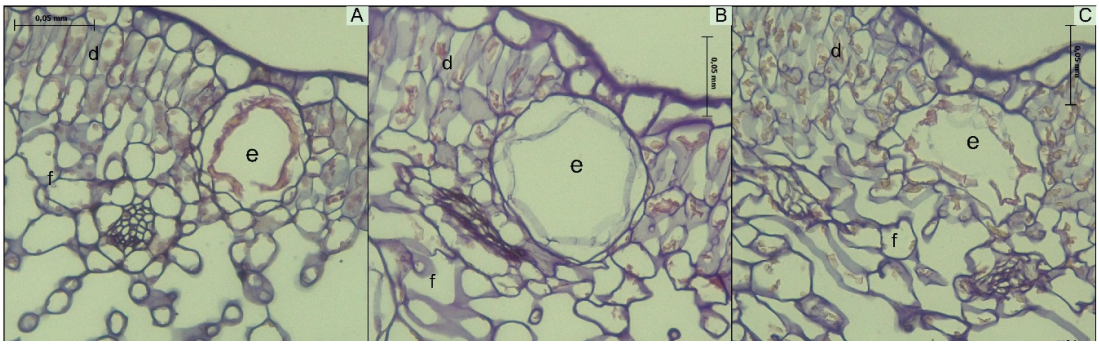

e. schizolysigenous cavities, d. palisade parenchyma, f. spongy parenchyma

Fig. 4. Micrography of the secretory cavities of the leaves of *Luma chequen* (*Molina*) *A. Gray* at different levels of moisture. (A-C) Cross sections of the leave at 50 μm: (A) Leave with 72% moisture, (B) Leave with 24% moisture, (C) leave with 8% moisture. Hematoxylin and eosin staining.

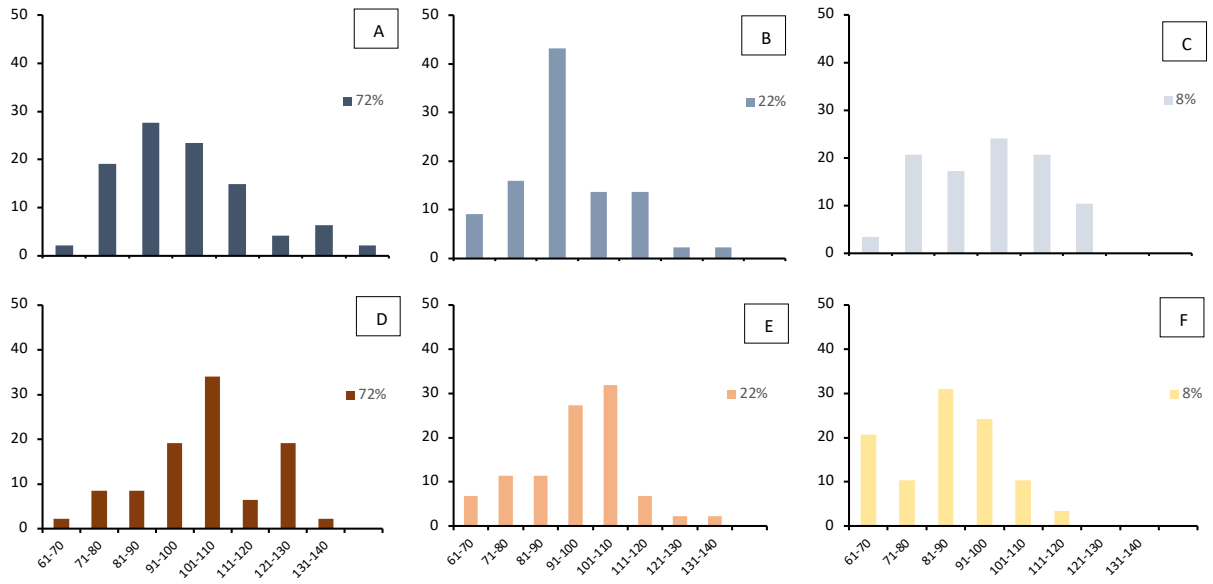

Fig 5. Size distribution of the secretory cavities contained in the leaves of *Luma chequen* (*Molina*) *A. Gray* with moisture levels of 72, 24 and 8%. Major diameters (A-C). Minor diameters (D-F). The x-axis intervals are in μm units.

Table 2. Ratio of major and minor diameters.

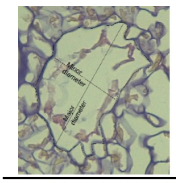

Moisture %	Average ratio (Dmajor/Dminor)	Standard deviation
72	1.2	0.2
24	1.3	0.3
8	1.7	0.3

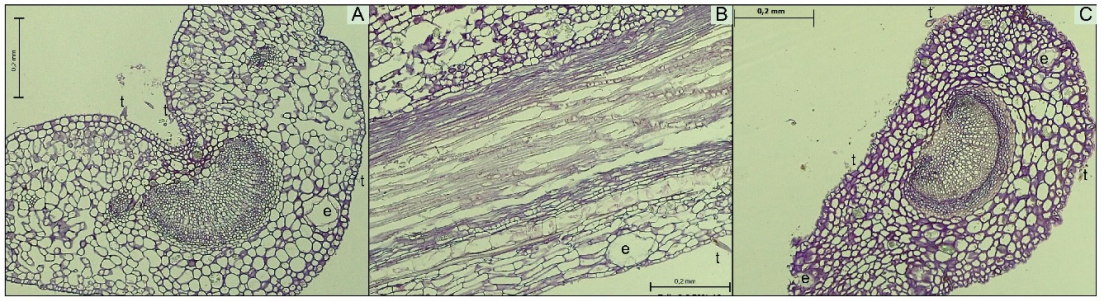

Fig. 6. Micrography of secretory cavities of young stems of *Luma chequen* (*Molina*) *A. Gray* at different levels of moisture. (A) Stem cross section at 72% moisture at 20 μm. (B) Longitudinal section of the stem at 72% moisture at 20 μm. (C) Cross section of the stem at 24% moisture at 20 μm. Hematoxylin and eosin staining.

This behaviour is also observed in Figures 5D, 5E and 5F, corresponding to the smaller diameters, with a much more skewed weight to the left. These trends show that the cavities may be reducing and, in some cases, collapsing, as a result of the folding caused by drying.

Likewise, Table 2 shows the average ratio of the largest to the smallest diameter of the secretory cavities observed in the samples of the 3 moisture levels, showing that the diameter ratio increases as the moisture decreases, indicating that, the cavities become thinner as the moisture decreases.

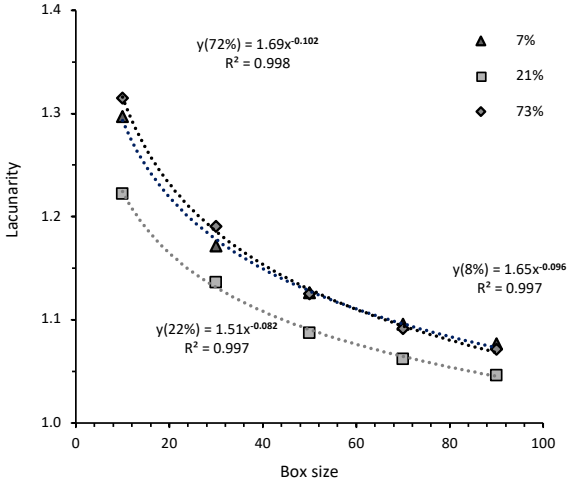

Fig. 7. Lacunarity curve of cross-sectional samples of leaves from *Luma chequen* (*Molina*) *A. Gray*, at moisture levels of 72%, 24% and 8%. Dotted lines represent polynomial fits.

These metrics hence allow us to detect the gradual geometric deformation of the cavities (Del Rosario *et al*., 2022).

Conversely, young stems also contain secretory cavities in the parenchymal tissue but in smaller proportion compared to leaves, as can be observed in the samples of young stems with 72% moisture, both in the cross section (Figure 6A) and longitudinal section (Figure 6B). The water loss in the stems occurs through their vascular tissue, mainly in the xylem (Rosner *et al*., 2019). In Figure 6C, at 24% moisture, it is shown that the secretory cavity preserves its shape. This could be the result of the protective action of the trichomes on the mesophyll (palisade and spongy parenchymal tissues) in an excessively hot atmosphere (Esau, 1982).

Estimation of lacunarity

In Figure 7 it is observed that as the size of the box is increased, the lacunarity decreases tending to 1, becoming more homogeneous as the observation scale is greater. A lacunarity value of 1 indicates that the object is completely uniform (Azor, 2016). Likewise, it can be noted that for the 24% moisture sample, the lacunarity values are lower, evidencing a lesser degree of disorder between the empty spaces. Clearly, the 8% moisture sample has higher lacunarity values due to the disorder of its structure generated by drying. However, the 72% sample shows values similar to the 8% sample, because in binary data, the intercellular fluids characteristic of the fresh state are observed in black, therefore, irregular spaces are seen inside the cells, in addition to epithelial cells surrounding the cavity being very well defined, creating additional voids.

Figure 7 shows that the curves approximately follow a power law, where the exponential values would characterize the cross section of the *Luma chequen* (*Molina*) *A. Gray* leaf at moisture levels of 72%, 24% and 8%, with values of -0.102, -0.082 and -0.096, respectively.

The fractal dimension of our samples was also estimated at different conditions but, consistent with Camelo *et al*. (2013) and Monroy *et al*. (2021), it was found that this parameter does not allow the identification of significant morphometric differences. The estimated value was 2.1, similar to that of the *Copaifera sp*. (Calla *et al*., 2016)

3.3 Relationship between moisture content and extraction yield

The experimental results of the relationship between the yield, expressed in terms of volume of oil per unit of mass (*v/w*) with the moisture content on wet basis of the vegetable material, are shown in Figure 8. The extraction yield is given by Eq. (3):

$$Yield(v/w) = \frac{v_{eo}}{W_{VM}} \times 100\% \qquad (3)$$

where, W_{VM} weight of vegetable material, g; and v_{eo} is volume of essential oil, ml.

In Figure 8A, the section on the left shows the increase in yield as the moisture of the plant material (X) decreases, following a y function, as shown in Eq. (4).

$$yield(v/w) = 0.00009X^2 - 0.0173X + 0.840 \qquad (4)$$

Also, from Figure 8B for this section we have Eq. (5), which relates the yield with the drying time (t).

$$yield(v/w) = 0.000006t^2 + 0.0007t + 0.0661 \qquad (5)$$

The maximum yield of 0.52 ± 0.01% (v/w) is reached at a moisture of 22% (Figure 8A) with a drying time of 225 minutes (Figure 8B). Beyond such a point, a decrease in yield is observed until the equilibrium moisture (8.2%) is reached, following a linear function. It is important to note that the moisture where maximum yield is achieved is very close to the critical moisture of 24±1%. That is, both the migration of water at 40 ° C and that of essential oil at 92 ° C from the interior of the plant material to the surface, decreases after arriving at the critical moisture.

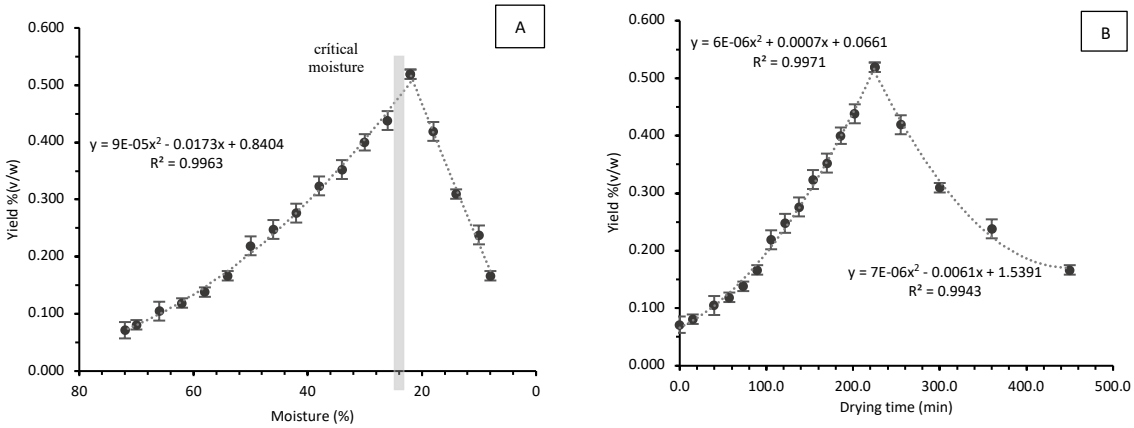

Fig. 8. Extraction yield of *Luma chequen* (*Molina*) *A. Gray* essential oil. (A) as a function of the moisture of the plant material. (B) as function of the drying time. The section on the left corresponding to the range from Xfresh to Xcr, and the section on the right, until Xeq. Dotted lines represent polynomial fits.

This turning point is reached at different temperatures, due to the difference in diffusivity of both the water and the volatile components of the essential oil. Indeed, Páramo *et al*. (2010) showed that the diffusivities of fatty acids are much lower than the diffusivity of water, as evidenced by a remaining acidity in the product dried at 40 ° C.

The optimal oil yield found in this study, 0.52% (v/w), lies within the range of [0.049-0.83%] (v/w) from previous studies by Fernández (2019), Moina (2015), and Ruiz *et al*. (2015) who also used steam distillation for the extraction of *Luma chequen* essential oil. The variability in the reported yields reflects differences in operation conditions like extraction times, steam pressure, and equipment size, as well differences in the parts of the plant used and their humidity. For *Myrtus Communis*, a similar plant species, a comparison of the ohmic-assisted hydrodistillation and steam distillation methods found that the yield was similar (0.66-0.67% v/w) with the former requiring less extraction time but producing a smaller content of α-Pineno (Gavahian *et al*., 2013). Also, for *Myrtus Communis*, a study comparing hydro-steam distillation and steam distillation found that the former gave a higher yield but the latter produced an essential oil with more active antibacterial effect (Dadazadeh and Nourafcan, 2021).

3.4 Extraction kinetics of the essential oil of Luma chequen

The kinetic of extraction was evaluated at the same way of Ismanto *et al*. (2018), comparing first and second kinetic models, because of it dealt with a species of the same botanic family.

Figure 9 shows the experimental curves for the extraction kinetics of the essential oil *Luma chequen* for vegetal material with different levels of humidity (72, 62, 50, 22, 14 y 8%), and the corresponding curves for first and second order kinetic models.

The first order kinetic model is based on the rate equation of Lagergren (1989);

$$\frac{dC_t}{dt} = k_1(C_s - C_t) \tag{6}$$

where k_1 is first-order rate constant (min^{-1}), C_S is the extraction capacity or concentration at saturation (gL^{-1}) and C_t is the concentration of oil extracted at time t (min). Integrating equation 6 yields:

$$\ln(C_s - C_t) = \ln(C_s) - k_1 t \tag{7}$$

Since best-fit values of C_S and k_1 cannot be found by straightforward linear regression, we found these values by searching for the minimum of the mean-squared error (MSE) when considering a series of preset values of C_S and associating to each such value the best estimator of k_1 based on the experimental data.

The second order kinetic model is based on rate equation (Ho *et al*., 2005):

$$\frac{dC_t}{dt} = k(C_s - C_t)^2 \tag{8}$$

where k is the second-order rate constant (L g^{-1} min^{-1}), and C_s and C_t have similar meaning as before. Equation (8) can be integrated and put in linear form as:

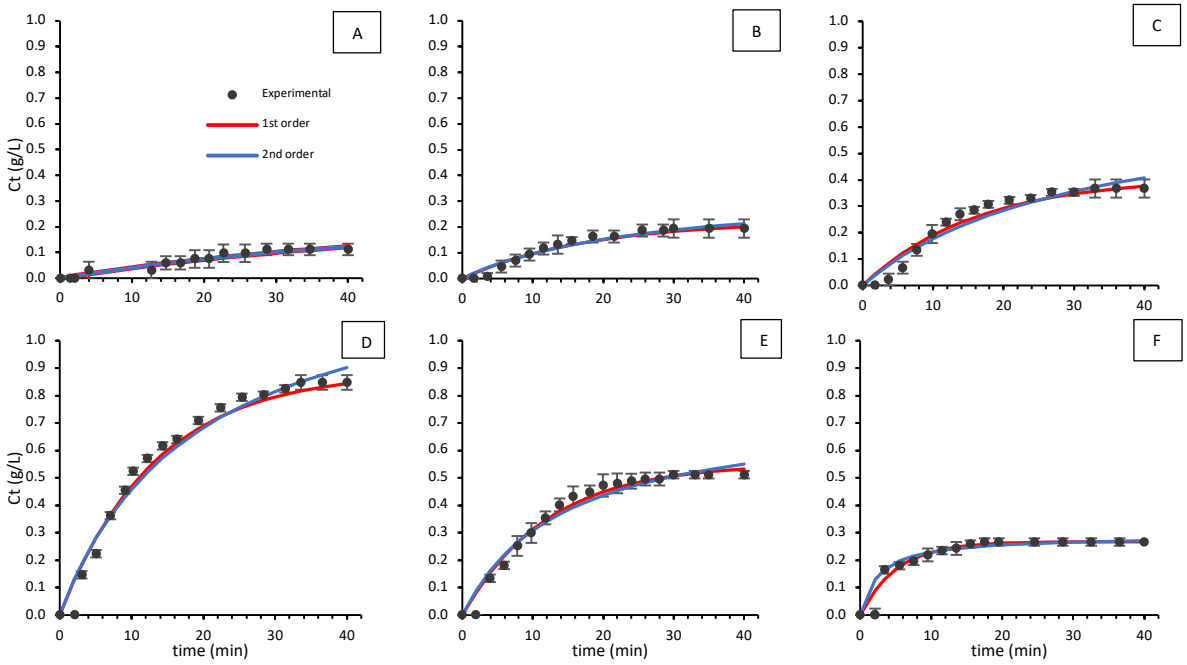

Fig. 9. Extraction kinetics of *Luma chequen* (*Molina*) *A. Gray* essential oil for samples of different humidity levels. (A) 72%. (B) 62%. (C) 50%. (D) 22%. (E) 14%. (F) 8%.

Table 3. Fit parameters of the first and second order kinetic models.

Moisture	First-order kinetic model					Second-order kinetic model				
%	Cs	K1	R^2	MSE	F cal	Cs	K	R^2	MSE	Fcal
72	0.222	0.02	0.946	0.0001	0.058	0.355	0.037	0.946	0.0001	0.058
62	0.224	0.057	0.963	0.0001	0.04	0.355	0.106	0.959	0.00022	0.044
50	0.42	0.059	0.954	0.00086	0.049	0.715	0.046	0.942	0.00109	0.062
22	0.888	0.075	0.979	0.00182	0.022	1.33	0.04	0.974	0.00305	0.028
14	0.551	0.084	0.978	0.00066	0.023	0.746	0.094	0.965	0.00105	0.037
8	0.272	0.157	0.904	0.00096	0.117	0.288	1.339	0.782	0.00216	0.232

$$\frac{t}{C_t} = \frac{1}{kC_s^2} + \frac{t}{C_s} \tag{9}$$

which allows the calculation of C_s and k from a t/C_t vs. t plot.

As can be seen in Table 3, the values of C_s for both models track the trend for the extraction yield for the different levels of humidity. The values of R^2 and MSE for both models are quite comparable for all cases (except for the 8% humidity level), with the first-order model exhibiting a slightly but consistently higher correlation. Application of the F-test with 95% confidence level reveals that both models are valid regressors of the data, with calculated F values smaller than threshold values (2.3 to 2.6). Figure 9 reveals that none of the two models is able to fit the data at short times, which likely reflects transient physical mechanisms that the models are not set to capture. For example, the diffusion of the vapor within the vegetable bed takes 1-2 min. and is part of the "lag time" that occurs between the moment the steam enters the unit until the moment the first distillate drop is detected. While the "zero" time for extraction kinetic analysis could be adjusted based on different criteria, the improvement on R^2 is marginal and hence the results presented can be seen as representative.

While on the basis of the numerical fits neither the

first nor second order model could be singled out as being significantly more suitable, the values and trends of the C_s and k_1/k values appear to be more physical for the first order model. Indeed, if one takes C_s to correspond to the yield that would be attainable at infinite extraction time, the values found for the 2nd order model appear to be too large. Likewise, while k_1 monotonically and gradually increases as the humidity level decreases (which would correlate with the effect of shorter diffusion lengths), the k values exhibit a non-monotonic trend and more disparate values. Note, however, that while a first-order model considers the diffusion within the solid to be the phenomenon determinant of the extraction kinetics (Meziane *et al.*, 2019), this describes an *effective* diffusion process, since, as discussed in Sec. 3.5, the extraction rate will depend on multiple factors such as level of exposure of the oil cavities, the dissolution and evaporation of the oil, etc.

3.5 Relationship between drying velocity and essential oil extraction

Multiple approaches have been used to model the drying of volatiles from porous materials. Different models involve different frameworks, some mechanistic others phenomenological, some incorporating heat transfer effects, others accounting for spatially anisotropic mass transfer (Katekawa and Silva, 2006; Kiranoudis *et al.*, 1992). Such models adopt specific assumptions regarding the system's geometry, homogeneity, and boundary conditions, and can be tailored to describe different length and times scales (Crank, 1975).

We only consider the case where the material is arranged in thin, highly porous beds so that the gas phase can readily flow through the bed and the main resistance to volatile mass transfer occurs at the level of individual leaves. Figure 10 illustrates two simple isothermal mechanistic models which are consistent with this premise, one based on an effective diffusivity (Fig. 10A) and the other based on effective interfaces (Fig. 10B). In the former model, intra-leave gradients are seen as the main driver of mass transfer, and drying curve data can be used to estimate the evolution of an *effective* intra-leaf diffusivity, while in the latter model the liquid-vapor interface represents the main resistance to mass transfer, and connections in oil evaporation rates can be looked at during both drying and extraction over periods when spatial concentration gradients are small. Key details and results from both models are summarized below:

1) Effective-diffusion model (Fig. 10A). At the level of a single leaf, the system can be approximated as a "slab" of thickness L whose internal gaseous compartments form an effectively pseudo-homogeneous medium where the humidity resides and "diffuses", primarily in a unidirectional manner (along x axis) toward the outer slab plane formed by the abaxial epidermis where the stomata are concentrated (see Fig. 3). In such a model, the effective diffusivity coefficient D_e embodies the concentration-gradient induced diffusion of moisture overcoming any resistance in both the vapor phase and through any internal interfaces. This process can then be described by Ficks' 2nd law of diffusion using as boundary conditions a constant concentration of humidity in the air stream passing over the abaxial surface and no flux condition at the adaxial epidermis plane, and as initial condition a slab with uniform composition.

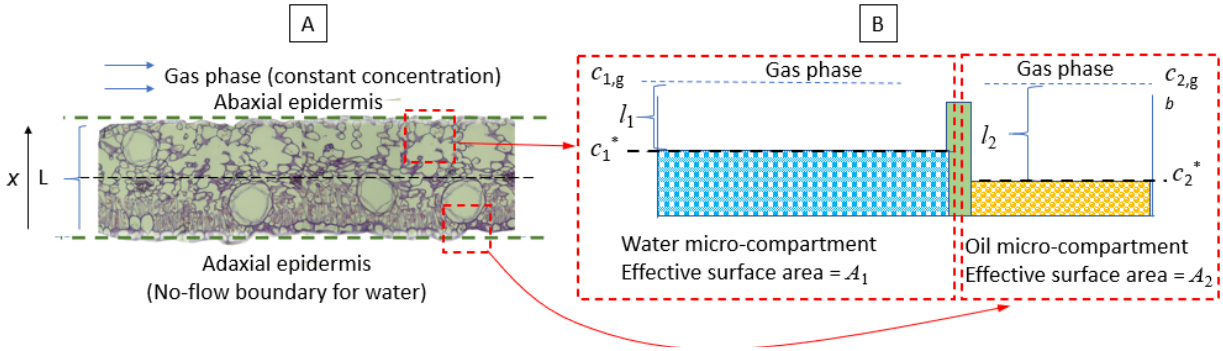

Fig. 10. Schematic representation of models used to analyze volatile mass transfer from a leaf to the gas phase. (a) Effective diffusion model where a leaf is approximated by an infinite slab model of pseudo-homogeneous material containing humidity, (b) Interfacial model illustrating compartments of water and essential oil.

A solution of this model and its application to the drying of our system is described in the Appendix. It is shown there that D_e for the humidity increases during the drying period, a trend that has also been reported in the drying of onion slices and banana foam mat (Pathare and Sharma, 2006; Thuwapanichayanan *et al*., 2008). Such an increase in D_e suggests that structural changes occur inside the leaves during drying which facilitate mass transfer; note, however, that the overall drying rate decreases as the concentration gradient decreases more rapidly. Moreover, such a variation in D_e is moderate (~ a factor of < 10 over the total drying period).2) Effective interfacial model (Fig. 10B). This model is primarily intended to describe the evaporation of essential oil in the open compartments inside the leaves. Unlike the previous model where evaporation was described as an effective concentration-driven process, this model takes explicitly into account the key physical mechanism responsible for the mass transfer resistance, the liquid-vapor boundary layer, contributing to any effective diffusivity. While liquid-phase diffusion, distributed evaporation models or serial compartments could be used to also account for spatial variations (Bartzanas *et al*., 2010; Datta, 2007), here we neglect such gradients and model representative "average" interfaces. We assume that the oil is pooled in small, accessible compartments and hence the main resistance to mass transfer is interfacial evaporation. This model is motivated by our experimental finding that, upon reaching critical drying conditions, the essential oil thereafter sustains large evaporative loses during drying. This suggests that under such conditions the essential oil has become more "interfacial", i.e., more exposed to the gas phase and prone to evaporation. In the following we detail this model and probe the relation between oil evaporation rates during air drying and steam extraction.

Based on an abstraction of the micromorphology of the material described above, in figure 10B the compartments for water (component 1) and essential oil (component 2) are represented separately. For simplicity, only one compartment per component is shown in this schematic, and the essential oil is represented as a single pseudocomponent. The evaporation rate for component i is shown in Eq. (10):

$$\frac{dN_i}{dt} = -A_i J_i \tag{10}$$

where N is number of moles, A is effective interfacial area and J is molar flux per unit area, which is given by Eq. (11) (Cussler, 1984):

$$J_i = \frac{D_i}{l_i}(c_i^* - c_{i,g}) \tag{11}$$

where D is diffusion coefficient in the boundary layer, l is the thickness of the boundary layer, c_i^* is molar concentration at the liquid-vapor interface and $c_{i,g}$ is concentration in the bulk of the gaseous mass flowing outside the interface. Note that D_i/l_i could also be expressed in terms of an effective mass transfer coefficient and that Eq. (11) constitutes the boundary evaporative condition for a diffusion equation model taking into account mass transfer resistance for the liquid to move up to the surface [in such a context, the prefactor in Eq. (11) averages out the effect of diffusivity in the liquid phase]. If we assume that such gas concentrations of volatiles are dilute and hence negligible relative to the concentration at saturation conditions c_i^* for both components during drying, and for oil during extraction; in such cases Equations (10) and (11) can be combined to give Eq. (12):

$$\frac{dN_i}{dt} = -\frac{A_i D_i}{l_i} c_i^* \tag{12}$$

Assuming that components 1 and 2 are insoluble in the liquid state, that the interfacial concentrations c_i^* correspond to the vapor in equilibrium with the liquid, and that the pressure is low, then Raoult and ideal gas laws can be combined to obtain Eq. (13):

$$c_i^* = (P_i^o(T))/RT \tag{13}$$

Where $P_i^0(T)$ is the saturation pressure of component i (whose dependence on temperature T is explicitly expressed) and R is the ideal gas constant. Equations (12) and (13) combine to give Eq. (14),

$$\frac{dN_i}{dt} = -\frac{A_i D_i}{R l_i} \frac{P_i^o(T)}{T} \tag{14}$$

As the right-hand side of Equation (14) is a constant for a given temperature and other external constant conditions, the model predicts a constant evaporation rate as long as internal morphological factors of the material (reflected in the values of A and l) do not change. While D and l could be estimated based on theoretical models, it would be very difficult to estimate the parameter A based on theory or experiment and hence to use Eq. (14) to make direct quantitative predictions. In the following we show how it is possible to productively use Eq. (14) for a semi-quantitative analysis which *does not* require the knowledge of individual parameters D and l.

Although model (14) could be applied to the drying of moisture over narrow periods when physical properties of the material are relatively constant, in the following we constrain its use to describe oil transfer during the drying and extraction operations.

Essential oil evaporation during drying

For component 2, the fact that the loss of essential oil is negligible before the critical drying point would be associated in the model with a very small value of A_2/l_2, corresponding to the very limited access to the oil compartments. After the critical point, the associated microstructural changes would lead to a drastic change in the A_2/l_2 factor that would generate a significant evaporation of the oil. In such a situation and as long as A_2/l_2 does not change, the oil drying speed must be constant and with a value given by:

$$\left(\frac{dN_2}{dt}\right)_{drying} = -\frac{A_2 D_2}{R l_2}\frac{P_2^o(313.1K)}{313.1K} \qquad (15)$$

This approximately constant slope regime is observed in Figure 8 for drying times greater than 225 min.

Essential oil evaporation during extraction of dried material

As the oil and moisture access interfaces of the material are different (as shown in Figure 3, where water is lost primarily through the stomata and oil through the beam), the initial water absorption during extraction should have minimal effect on oil evaporation. Consistent with the previous analysis, the evaporative velocity for samples whose moisture was not reduced to the critical value, would have small values of A_2/l_2 that produce negligible evaporation during drying (at 40 ºC) and slow oil extraction (at 92.2 ºC).

The relevance of model (14) is most clearly revealed by applying it to the initial period of essential oil extraction from samples that were dried to or beyond the critical point. It is assumed that microstructural changes caused to the oil compartments at the critical point are irreversible so that the parameters A_2/l_2 associated with the evaporation of oil by drying [and that appear in Eq. (15)] are the same as those that act during the oil evaporation in extraction. Then applying model (15) to the extraction temperature of ~ 92.2 ºC = 365.3 K:

$$\left(\frac{dN_2}{dt}\right)_{extraction} = -\frac{A_2 D_2}{R l_2}\frac{P_2^o(365.3K)}{365.3K} \qquad (16)$$

Comparing (15) and (16), it is expected that A_2 is the same and that the change in the ratio D_2/l_2 is small between 40 ºC and 92 ºC, therefore, these relationships can be combined to give Eq. (17):

$$\frac{(dN_2)/dt)_{extraction}}{(dN_2)/dt)_{drying}} \approx \frac{P_2^o(365.3K)/365.3K}{P_2^o(313.1K)/313.1K} \qquad (17)$$

The right-hand side of Equation (17) can be evaluated using Antoine's equation for alpha-pinene (as the most abundant and representative component of essential oil) (Hawkinds and Armstrong, 1954). The left side of Equation (17) can be estimated based on the post-critical linear portion of Figure 8B (for the denominator) and the first linear portion of the extraction after the initial non-stationary period of a sample dried to the critical point, considering the 22% moisture of Figure 9 (for the numerator). The result is:

$$\frac{-(0.352-0.090)\%)/(12.2-3.1)min}{(0.519-0.310)\%)/(225-300)min} \approx \frac{0.1447bar/365.3K}{0.0139bar/313.1K}$$

$$10.2 \approx 8.9$$

The proximity between these values supports the model presented and is consistent with the expectation that *the same evaporation mechanism governs both processes*: the loss of oil in drying and the subsequent extraction of oil in the dried samples. In effect, this analysis demonstrates how, for certain conditions, drying data could be used to make predictions of initial steam distillation kinetics. On the other hand, the model does not directly capture the delay in the extraction velocity at longer times that reflect changes in the accessibility to residual oil compartments (i.e., changes in A_2/l_2).

Consistent with this finding, for the *Eucalyptus globulus* species, also belonging to the *Myrtaceae* family, Moreno (2010) reports that the optimal range of humidity of the plant material, which is subjected to extraction of essential oil by steam distillation, varies from 25 to 30% and the critical humidity is 34.35%, also demonstrating the proximity between the mentioned values.

3.6 Composition of the essential oil of Luma chequen (Molina) A. Gray

The analysis of CG-MS performed for the sample of vegetable material with 22% moisture presents a proportion of monoterpenes of 70.8%, among which, the following components may be found in higher proportion: α-pinene, 1,8-cineole, limonene, β-pinene

and linalool (Table 4); and 18.1% of sesquiterpenes, standing out the selinenes: α-Selinen, β-Selinen and δ-Selinen (10.9%). In contrast to what Gonçalvez *et al*. (2011) and Vallverdú *et al*. (2006) report, parity between non-oxygenated monoterpenes was observed, with the exception of α-pinene, which is present in a proportion smaller to the 57% found in these studies. Incidentally, this is the component of lowest boiling point of non-oxygenated monoterpenes present in the sample. In consequence, it is presumed that part of the α-pinene was lost during the drying process due to that fact that studies show that monoterpenes tend to exit through the adaxial epidermis (beam), especially those located in cavities closer to the surface (Guenther, 1991).

Table 4. Composition of the sample of *Luma chequen* (*Molina*) *A. Gray* essential oil with 22% moisture.

t_R, **min**	**linear retention rates, LRR**		**Tentative identification**	**Relative quantity**
DB-5MS	**DB-5MS**	**DB-WAX**		**%**
	915	1092	2-methylpropyl 2-Methylpropanoate	1.5
16,38	929	1025	α-Thujene	0.3
16,78	938	1022	α-Pinene	44
17,53	954	1065	Camphene	0.4
18,77	982	1108	β-Pinene	4.7
19,68	1003	1177	2-methylpropyl 2-Methylbutanoate	0.5
20,10	1013	1195	3-methylbutyl 2-Methylpropanoate	0.6
20,24	1016	1198	2-methylbutyl 2-Methylpropanoate	2.3
20,77	1029	1270	p-Cymene	1.1
20,98	1034	1198	Limonene	4.7
21,15	1038	1211	1,8-Cineole	9.4
22,19	1063	1245	γ-Terpinene	0.8
23,34	1090	1283	Terpinolene	0.3
23,81	1102	1546	Linalool	2.7
23,91	1104	1282	2-methylbutyl 2-Methylbutanoate	0.5
26,91	1181	1706	Borneole	0.4
27,19	1188	-	Terpinen-4-ol	0.3
27,72	1202	1700	α-Terpineol	1.7
36,27	1434	1605	Trans-β-Caryophyllene	1.6
38,02	1485	1680	Eudesma-4(14),7(11)-diene (δ-Selinen)	1.1
38,64	1503	1725	β-Selinen	4.7
38,84	1510	1729	α-Selinen	5.1
39,40	1528	1758	δ-Cadinene	0.4
39,89	1544	-	Flavesone	0.4
41,53	1599	1990	Caryophyllene oxide	1.1
41,60	1601	2080	Globulol	0.5
41,89	1612	2059	Cubeban-11-ol	0.6
43,42	1669	2236	α-Cadinol	0.5
43,60	1676	2259	Selin-11-en-4a-ol	2.4
			Monoterpenes	56.3
			Oxygenated monoterpenes	14.5
			Sesquiterpenes	12.9
			Oxygenated sesquiterpenes	5.1
			Others	5.8
			Total identified	94.6

On the other hand, it can be noted that the content of sesquiterpenes is high (18.1%) with respect to the values obtained in the aforementioned studies, 2.9% and 3.1%. High concentrations of sesquiterpenes were also evidenced in the essential oil of *Eugenia uniflora*, obtained from material dried at a temperature of 45°C (Alves de Assis *et al*., 2020). It should be mentioned that the vapor entry pressure of 34.5 kPa would have favored the extraction of sesquiterpenes (components with higher molecular weight). Also, a high content of these components could improve the antioxidant property of essential oil (Stashenko *et al*., 2003).

Conclusions

A comprehensive study was conducted on the steam-distillation extraction of the essential oil from *Luma chequeen*. Besides characterizing the extract composition, our analyses included the morphological evaluation of the leaves and stems, the assessment of the effect of the humidity level on the extraction yield, and the modeling of the extraction kinetics, elucidating the connection between extraction and oil evaporation rates.

The micromorphological evaluation of the leaves and young stems of *Luma chequen* (*Molina*) *A. Gray* reveals that drying causes folding in the tissue surrounding the secretory cavities, thus reducing the structural barrier for the exit of essential oil. The ratio of cavity diameters increases from 1.2 to 1.7, as the moisture decreases from 72±1%, in the fresh state, to the equilibrium moisture of 8.2±0.5%, evidencing the thinning of the cavities. According to the lacunarity, the cross sections of the *Luma chequen* leaves present exponential values that characterize them; between -0.102 and -0.082; and the sample at the critical moisture of 24±1 presents the highest degree of order, forboding a favorable microstructural change at this moisture level.

A maximum yield of 0.52±0.01% (v / w) was achieved in the extraction of the essential oil of *Luma chequen* (*Molina*) *A. Gray* when the moisture of the plant material is 22% (225 min drying at 40 ° C), close to critical humidity (24±1%). First and second order models were fitted to the experimental extraction kinetic data and found that while both models provide statistically significant regressions, the first order model was found to provide not only slightly better fit to the data, but also more physical values for the fitting parameters (rate constant and saturation capacity). The optimal conditions found here for oil extraction yield are also associated with fast kinetics and hence relatively short processing times, which can potentially translate into reduced energetic consumption per unit weight of product.

A mathematical model was introduced that supports the tenet that oil evaporation represents the main resistance for oil mass transfer during both the drying of the material (causing oil losses) and steam-distillation extraction for cases when the sample was dried at (or beyond) the critical humidity. Therefore, from the kinetics of drying one could predict the early, linear portion of the essential oil extraction kinetics. It is posited that a similar predictive drying-extraction-rate connection could be applicable to other species with micro-morphologies and essential oil compositions similar to those of *Luma chequen*.

The monoterpenes components α-pinene, 1,8-cineole, limonene, β-pinene y linalool of essential oil, which correspond to the extraction test with highest yield (22% moisture), are in the ratio of 44%, 9.4%, 4.7%, 4.7% and 2.7%, respectively, preserving the components with known pharmacological properties. Likewise, it contains sesquiterpenes (18.1%) in proportions greater than reported in other studies.

Acknowledgments

The authors would like to acknowledge the financial support granted to this research project by the Universidad Nacional de San Agustin de Arequipa (UNSA) through the contract Nº TP-019-2018-UNSA. The authors would also like to acknowledge the valuable contribution of Dr. Luis Felipe Miranda Zanardi in the development and critical revision of this work.

Appendix

Macroscopic model solution. The solution of the diffusion equation for the boundary and initial conditions and slab geometry outlined in Sec. 3.4 and Fig. 10A is given by (Crank, 1975):

$$MR = \frac{X_t - X_e}{X_0 - X_e} = \frac{8}{\pi^2} \sum_{n=0}^{\infty} \frac{1}{(2n+1)^2} \exp\left[-(2n+1)^2 \pi^2 \frac{D_e}{L^2} t\right] \tag{A1}$$

where MR is the fractional residual humidity, X_t is the humidity constant at time t, X_0 is the initial humidity content, X_e is the humidity at equilibrium, n is a positive integer, D_e is the effective diffusivity of the

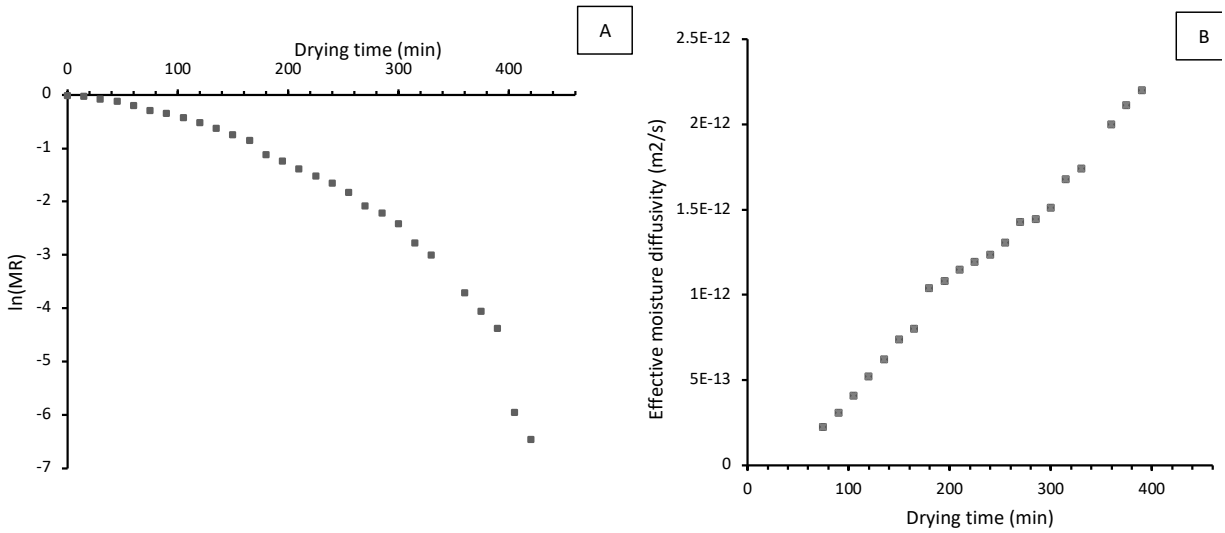

Fig. 11. A. Variation of ln (MR) as a function of drying time. B. Effective moisture diffusivity as a function of drying time at 40°C

humidity through the material (m^2s^{-1}), t is time (s), and L is the thickness of the hypothetical slab (m), which is twice the thickness of a leaf to exploit the symmetric solution (which is symmetric around the hypothetical slab center-plane where the no-flux boundary condition applies).

For long drying periods, la Eq. (A1) simplifies to the first term in the series,

$$\ln(MR) = \ln\left(\frac{8}{\pi^2}\right) - \left(\frac{\pi^2 D_e}{L^2}\right)t \qquad \text{(A2)}$$

Equation (A2), based on the assumption of a constant D_e at the given temperature, predicts a linear relation between the logarithm of the residual humidity and time. However, Figure 11A shows that this relationship is not linear, in which case the values of D_e can be estimated by the method of slopes (Karathanos *et al*., 1990), for fixed L.

$$D_e = \frac{\left(\frac{dMR}{dt}\right)_{exp}}{\left(\frac{dMR}{dF_0}\right)_{th}} L^2 \qquad \text{(A3)}$$

where F_0 is Fourier's number given by $F_0 = D_e t/L^2$ (Pathare and Sharma, 2006), so that Eq. (A2) can be rewritten as

$$MR = \frac{8}{\pi^2}\exp(-\pi^2 F_0) \qquad \text{(A4)}$$

where:

$$F_0 = -0.101 \ln M_R - 0.0213 \qquad \text{(A5)}$$

and D_e can be calculated from:

$$D_e = \frac{F_0}{t/L^2} \qquad \text{(A6)}$$

The value of L was 0.35 ± 0.05 mm. As can be observed in Fig. 11B, D_e varies during the drying period. This analysis indicates that the drying process can be seen as a sequence of short pseudo-steady state regimes where in each regime De and related physical properties remain unchanged.

References

Allain C. and Cloitre M. (1991). Characterizing the lacunarity of random and deterministic fractal sets. *Physical Review A 44*, 3552. https://doi.org/10.1103/PhysRevA.44.3552

Alves de Assis, A. L., Raupp Cipriano, R., Lorena Cuquel, F., and Deschamps, C. (2020). Effect of drying method and storage conditions on the essential oil yield and composition in *Eugenia uniflora L.* leaves. *Revista Colombiana de Ciencias Hortícolas 14*(2). https://doi.org/10.17584/rcch.2020v14i2.9281

An, K., Zhao, D., Wang, Z., Wu, J., Xu, Y., and Xiao, G. (2016). Comparison of different drying methods on Chinese ginger (*Zingiber officinale Roscoe*): Changes in volatiles, chemical profile,

antioxidant properties, and microstructure. *Food Chemistry 197*, 1292-1300. https://doi.org/10.1016/j.foodchem.2015.11.033

Arenas, E. (2010). Técnica Histológica. [En línea]. Available: http://bct.facmed.unam.mx/wpcontent/uploads/2018/08/3_tecnica_histologica.pdf

Azor, J. R. (2016). El concepto de Lacunaridad como incentivo en la vinculación de la estadística y la informática con la ingeniería. En Álvarez, Ingrith; Sua, Camilo (Eds.), *Memorias del II Encuentro Colombiano de Educación Estocástica* (pp. 168-176). Bogotá, Colombia. http://acedest.org/2-encuentro/docs/Memorias_2ECEE.pdf

Bartzanas, T., Bochtis, D. D., Sørensen, C. G., Sapounas, A. A. and Green, O. (2010). A numerical modelling approach for biomass field drying. *Biosystems Engineering 106(4)*, 458-469. https://doi.org/10.1016/j.biosystemseng.2010.05.010

Berka-Zougali, B., Hassani, A., Besombes, C., and Allaf, K. (2010). Extraction of essential oils from Algerian myrtle leaves using instant controlled pressure drop technology. *Journal of Chromatography A 1217(40)*, 6134-6142. https://doi.org/10.1016/j.chroma.2010.07.080

Boutebouhart, H., Didaoui, L., Tata, S., and Sabaou, N. (2019). Effect of extraction and drying method on chemical composition, and evaluation of antioxidant and antomicrobial activities of essential oils from *Salvia officinalis L. Journal of Essential Oil Bearing Plants 22(3)*, 717-727. https://doi.org/10.1080/0972060X.2019.1651223

Cabrera, C. E. (2019). Actividad antimicrobiana de un sistema a base de un extracto vegetal y tres aceites esenciales. *Ciencia e Investigación 22(1)*, 21-25. https://doi.org/10.15381/ci.v22i1.16811

Calla, M. O., Zamora, R. R. M., and Carvalho, J. C. T. (2016). Estudio fractal de la superficie de la hoja de la especie vegetal *Copaifera sp*. haciendo uso del microscopio de fuerza atómica-AFM. *Revista ECIPerú 13(1)*, 7-7. https://doi.org/10.33017/RevECIPeru2016.0002/

Camelo-Méndez, G. A., Vanegas-Espinoza, P. E., Jiménez-Aparicio, A. R., Bello-Pérez, L. A., and Villar-Martínez, D. (2013). Morphometric characterization of chalkiness in Mexican rice varieties by digital image analysis and multivariate discrimination. *Revista Mexicana de Ingeniería Química 12(3)*, 371-378. https://doi.org/10.24275/rmiq/Bio2407

Carhuapoma Yance, M., Bonilla R., P., Suarez C., S., Villa, R., and López G., S. (2006). Estudio de la composición química y actividad antioxidante del aceite esencial de *Luma chequen* (*Molina*) *A. Gray* "Arrayán". *Ciencia e Investigación 8(2)*, 73-79. https://doi.org/10.15381/ci.v8i2.5306

Chávez-Magdaleno, M. E., Luque-Alcaraz, A. G., Gutierrez-Martínez, P., Cortez-Rocha, M. O., Burgos-Hernández, A., Lizardi-Mendoza, J., and Plascencia-Jatomea, M. (2018). Effect of chitosan-pepper tree (*Schinus Molle*) essential oil biocomposites on the growth kinetics, viability and Membrane integrity of *Colletotrichum gloeosporioides*. *Revista Mexicana de Ingeniería Química 17(1)*, 29-45. https://doi.org/10.24275/uam/izt/dcbi/revmexingquim/2018v17n1/Chavez

Ciccarelli, D., Garbari, F., and Pagni, A. M. (2008). The flower of Myrtus communis (*Myrtaceae*): Secretory structures, unicellular papillae, and their ecological role. *Flora-Morphology, Distribution, Functional Ecology of Plants 203(1)*, 85-93. https://doi.org/10.1016/j.flora.2007.01.002

Crank J. 1975. *The Mathematics of Diffusion*. 2nd ed. Oxford, UK: Clarendon Press.

Cussler E.L. (1984). *Diffusion: Mass Transfer in Fluid Systems*. New York: Cambridge University Press.

Dadazadeh, A., and Nourafcan, H. (2021). The effect of different essential oil extraction methods on the efficiency and antibacterial properties of *Myrtus Communis L.* leaves. *International Journal of Modern Agriculture 10(2)*, 4762-4775. http://modern-journals.com/index.php/ijma/article/view/1448

Datta, A. K. (2007). Porous media approaches to studying simultaneous heat and mass transfer

in food processes. I: Problem formulations. *Journal of Food Engineering 80(1)*, 80-95. https://doi.org/10.1016/j.jfoodeng.2006.05.013

Dávila, J. (2004). Estudio experimental del efecto de la porosidad de partículas sobre lecho fluidizado a vacío empleando aire. Tesis de Licenciatura, Universidad de las Américas - Puebla, Puebla. Colección de Tesis Digitales. http://catarina.udlap.mx/u_dl_a/tales/documentos/lim/davila_n_jr/

Del Rosario-Santiago, J., Ruiz-Espinosa, H., Ochoa-Velasco, C. E., Escobedo-Morales, A., and Ruiz-López, I. I. (2022). Effect of shrinkage and concentration basis on water diffusivity estimation and oil transfer during deep-fat frying of foods. *Revista Mexicana de Ingeniería Química 21(1)*, Alim2667-Alim2667. https://doi.org/10.24275/rmiq/Alim2667

Dima, C., and Dima, S. (2015). Essential oils in foods: extraction, stabilization, and toxicity. *Current Opinion in Food Science 5*, 29-35. https://doi.org/10.1016/j.cofs.2015.07.003

Esau, K. (1982). Anatomía de las Plantas con semilla. California, Estados Unidos: Hemisferio Sur. http://www.agro.unc.edu.ar/~wpweb/botaxo/wp-content/uploads/sites/14/2016/08/Esau_Anatomia_de_las_plantas_con_semilla.pdf

Fernández, L. (2019). Principios activos del aceite esencial de *Luma chequen* (*Molina*) *A. Gray* "Arrayan" y evaluación de su actividad antibacteriana. Tesis de Doctorado, Universidad Nacional de San Agustín de Arequipa, Arequipa. Repositorio Institucional de UNAS. http://repositorio.unsa.edu.pe/handle/UNSA/9290

Freire, J. T., Da Silveira, A. M., and do Carmo Ferreira, M. (2012). *Transport Phenomena in Particulate Systems*. Bentham Science Publishers. https://doi.org/10.2174/97816080522711120101

Gavahian, M., Farahnaky, A., Javidnia, K., and Majzoobi, M. (2013). A novel technology for extraction of essential oil from Myrtus communis: ohmic-assisted hydrodistillation. *Journal of Essential Oil Research 25(4)*, 257-266. https://doi.org/10.1080/10412905.2013.775676

Gonçalves, M. J., Cavaleiro, C., Proença da Cunha, A., and Salgueiro, L. R. (2011). Chemical composition and antimicrobial activity of the commercially available oil of *Luma chequen*. *Journal of Essential Oil Research 18(1)*, 108-110. https://doi.org/10.1080/10412905.2006.9699402

Guenther, A. B., Monson, R. K., and Fall, R. (1991). Isoprene and monoterpene emission rate variability: observations with eucalyptus and emission rate algorithm development. *Journal of Geophysical Research: Atmospheres 96(D6)*, 10799-10808. https://doi.org/10.1029/91JD00960

Hawkinds, J.E. and Armstrong, G.T. (1954). Physical and thermodynamic properties of terpenes. III. The vapor pressures of α-pinene and β-pinene. *Journal of the American Chemical Society 76*, 3756-3759. https://doi.org/10.1021/ja01643a051

Ho, Y. S., Harouna-Oumarou, H. A., Fauduet, H., and Porte, C. (2005). Kinetics and model building of leaching of water-soluble compounds of Tilia sapwood. *Separation and Purification Technology 45(3)*, 169-173. https://doi.org/10.1016/j.seppur.2005.03.007

Karathanos,V. T.,Villalobos,G.,and Saravacos,G. D. (1990). Comparison of two methods of estimation of the effective moisture diffusivity from data. *Journal of Food Science 55(1)*, 218-231. https://doi.org/10.1111/j.1365-2621.1990.tb06056.x

Katekawa, M. E., and Silva, M. A. (2006). A review of drying models including shrinkage effects. *Drying Technology 24(1)*, 5-20. https://doi.org/10.1080/07373930500538519

Kiranoudis, C. T., Maroulis, Z. B., and Marinos-Kouris, D. (1992). Model selection in air drying of foods. *Drying Technology 10(4)*, 1097-1106. https://doi.org/10.1080/07373939208916497

Kusuma, H. S., and Mahfud, M. (2017). The extraction of essential oils from patchouli leaves (*Pogostemon cablin Benth*) using a microwave air-hydrodistillation method as a new green

technique. *RSC Advances 7(3)*, 1336-1347. https://doi.org/10.1039/C6RA25894H

Kusuma, H. S., and Mahfud, M. (2018). Kinetic studies on extraction of essential oil from sandalwood (*Santalum album*) by microwave air-hydrodistillation method. *Alexandria Engineering Journal 57(2)*, 1163-1172. https://doi.org/10.1016/j.aej.2017.02.007

Ismanto, A. W., Kusuma, H. S., and Mahfud, M. (2018). Solvent-free microwave extraction of essential oil from *Melaleuca leucadendra L.* In MATEC Web of Conferences (Vol. 156, p. 03007). EDP Sciences. https://doi.org/10.1051/matecconf/201815603007

Masango, P. (2005). Cleaner production of essential oils by steam distillation. *Journal of Cleaner Production 13*, 833-839. https://doi.org/10.1016/j.jclepro.2004.02.039

McCabe, W. L., and Smith, J. C. (2007). *Operaciones Unitarias en Ingeniería Química*. México: McGraw-Hill/Interamericana Editores.

Meziane, I. A., Bali, N., Belblidia, N. B., Abatzoglou, N., and Benyoussef, E.-H. (2019). The first-order model in the simulation of essential oil extraction kinetics. *Journal of Applied Research on Medicinal and Aromatic Plants 15*, 100226. https://doi.org/10.1016/j.jarmap.2019.100226

Moina, V. (2015). Actividad antibacteriana *in vitro* de colutorios elaborados con aceites esenciales de *Luma chequen A. Gray* "Arrayán" y Mintostachis spicata (Benth). Epling "Yuraq Muña" frente a la cepa *Streptococcus mutans* ATCC 25175. Cusco: Universidad Nacional de San Antonio de Abad del Cuzco. Repositorio Institucional - UNSAAC. http://repositorio.unsaac.edu.pe/bitstream/handle/20.500.12918/146/253t20150050.pdf?sequence=1&isAllowed=y

Moghrani, H., and Maachi, R. (2008). Valorization of *Myrtus communis* essential oil obtained by steam driving distillation. *Asian Journal of Scientific Research 1(5)*, 518-524. https://doi.org/10.3923/ajsr.2008.518.524

Monroy-Rodríguez, I., Gutiérrez-López, G. F., Hernández-Sánchez, H., López-Hernández, R. E., Mazón, M. C., Dorántes-Álvarez, L., and Alamilla-Beltrán, L. (2021). Surface roughness and textural image analysis, particle size and stability of microparticles obtained by microfluidization of soy protein isolate aggregates suspensions. *Revista Mexicana de Ingeniería Química 20(2)*, 787-805. https://doi.org/10.24275/rmiq/Alim2311

Montoya Cadavid, G. d. (2010). *Aceites esenciales. Una Alternativa de Diversificaión para el Eje Cafetero* (Primera Edición ed.). Manizales: Universidad Nacional de Colombia. https://repositorio.unal.edu.co/bitstream/handle/unal/55532/9588280264.pdf?sequence=1&isAllowed=y

Moreno, J. C., López, G., and Siche, R. (2010). Modelación y optimización del proceso de extracción de aceite esencial de Eucalipto (*Eucaliptus globulus*). *Scientia Agropecuaria 1(2)*, 147-154. http://dx.doi.org/10.17268/sci.agropecu.2010.02.05

Muchtar, M., Suciati, N., and Fatichah, C. (2016). Fractal dimension and lacunarity combination for plant leaf classification. *Jurnal Ilmu Komputer dan Informasi 9(2)*, 96-105. https://doi.org/10.21609/jiki.v9i2.385

Páramo, D., García-Alamilla, P., Salgado-Cervantes, M. A., Robles-Olvera, V. J., Rodríguez-Jimenes, G. C., and García-Alvarado, M. A. (2010). Mass transfer of water and volatile fatty acids in cocoa beans during drying. *Journal of Food Engineering 99(3)*, 276-283. https://doi.org/10.1016/j.jfoodeng.2010.02.028

Pathare, P. B., and Sharma, G. P. (2006). Effective moisture diffusivity of onion slices undergoing infrared convective drying. *Biosystems Engineering 93(3)*, 285-291. https://doi.org/10.1016/j.biosystemseng.2005.12.010

Prophet, E., Mills, B., Arrington, J., Leslie, M. and Sobin, H. (1995). *Métodos Histotecnológicos*. Washington. Registro de Patología, 55-59.

Ramos, I. N., Brandão, T. R., and Silva, C. L. M. (2003). Structural changes during air drying of fruits and vegetables. *Food Science and Technology International 9(3)*, 201-206. https://journals.sagepub.com/doi/abs/10.1177/1082013030335522

Retamales, H. A., and Scharaschkin, T. (2015). Comparative leaf anatomy and micromorphology of the Chilean Myrtaceae: Taxonomic and ecological implications. *Flora-Morphology, Distribution, Functional Ecology of Plants 217*, 138-154. https://doi.org/10.1016/j.flora.2015.10.005

Reynel, C., and Marcelo, J. (2009). Árboles de los ecosistemas forestales andinos. Manual de identificación de especies. Lima, Perú: Serie de Investigación y sistematización No. 9. Programa Regional ECONOBA - INTERCOOPERATION. https://issuu.com/helicongus/docs/arboles_de_los_ecosistemas_forestal

Rezzoug, S. A., Boutekedjiret, C., and Allaf, K. (2005). Optimization of operating conditions of rosemary essential oil extraction by a fast controlled pressure drop process using response surface methodology. *Journal of Food Engineering 71(1)*, 9-17. https://doi.org/10.1016/j.jfoodeng.2004.10.044

Rosner, S., Heinze, B., Savi, T., and Dalla-Salda, G. (2019). Prediction of hydraulic conductivity loss from relative water loss: new insights into water storage of tree stems and branches. *Physiologia Plantarum 165(4)*, 843-854. https://doi.org/10.1111/ppl.12790

Ruiz, C., Díaz, C., and Rojas, R. (2015). Composición química de aceites esenciales de 10 plantas aromáticas peruanas. *Revista de la Sociedad Química del Perú 81(2)*, 81-94. https://doi.org/10.37761/rsqp.v81i2.10

Salcedo-Mendoza, J. G., Contreras-Lozano, K., García-López, A., and Fernandez-Quintero, A. (2016). Modelado de la cinética de secado del afrecho de yuca (*Manihot esculenta Crantz*). *Revista Mexicana de Ingeniería Química 15(3)*, 883-891. http://rmiq.org/iqfvp/Pdfs/Vol.%2015,%20No.%203/Alim10/Alim10.html

Santacruz-Vázquez, V., Santacruz-Vázquez, C., Welti-Chanes, J., Farrera-Rebollo, R. R., Alamilla-Beltrán, L., Chanona-Pérez, J., and Gutiérrez-López, G. F. (2008). Effects of air-drying on the shrinkage, surface temperatures and structural features of apples slabs by means of fractal analysis. *Revista Mexicana de Ingeniería Química 7(1)*, 55-63. http://rmiq.org/iqfvp/Pdfs/Vol%207%20no%201/RMIQ_Vol7No1_7.pdf

Sotta, N. (2000). *Plantas Aromáticas y Medicinales de la Región Arequipa*. Arequipa, Perú: ONG El Taller.

Stashenko, E. E., Jaramillo, B. E., and Martínez, J. R. (2003). Comparación de la composición química y de la actividad antioxidante in vitro de los metabolitos secundarios volátiles de plantas de la familia Verbenaceae. *Revista de la Académica Colombiana de Ciencias Exactas, Físicas y Naturales 27(105)*, 579-597. https://repositorio.accefyn.org.co/jspui/bitstream/001/594/1/105.pdf#page=105.

Stratakos, A. C., and Koidis, A. (2016). Methods for extracting essential oils. *Essential Oils in Food Preservation, Flavor and Safety*, 31-38. doi: 10.1016/b978-0-12-416641-7.00004-3

Talati, A. (2012) *Extraction Methods of Natural Essential Oils*. https://doi.org/10.13140/RG.2.2.18744.34564

Thuwapanichayanan, R., Prachayawarakorn, S., and Soponronnarit, S. (2008). Drying characteristics and quality of banana foam mat. *Journal of Food Engineering 86(4)*, 573-583. https://doi.org/10.1016/j.jfoodeng.2007.11.008

Vallverdú, C., Vila, R., Tomi, F., Carhuapoma, M., and Casanova, J. (2006). Composition of the essential oil from leaves and twigs of *Luma chequen*. *Flavour and Fragance Journal 21(2)*, 241-243. https://doi.org/10.1002/ffj.1565

Vieira de Souza, A. V., de Brito, D., Soares dos Santos, U., dos Passos Bispo, L., Casanova Turatti, I. C., Peporine Lopes, N. and Guedes da Silva Almeida, J. R. (2016). Influence of season, drying temperature and extraction time on the yield and chemical composition of 'marmeleiro' (*Croton sonderianus*) essential oil. *Journal of Essential Oil Research 29(1)*, 76-84. https://doi.org/10.1080/10412905.2016.1178183